Published in Optics Express, 23, issue 17, 21836-21856, 2015
which should be used for any reference to this work

Frequency comb offset dynamics of SESAM modelocked thin disk lasers

Florian Emaury,[1,3,*] Andreas Diebold,[1,3] Alexander Klenner,[1] Clara J. Saraceno,[1,2] Stéphane Schilt,[2] Thomas Südmeyer,[2] and Ursula Keller[1]

[1]*ETH Zurich, Institute for Quantum Electronics, Auguste-Piccard-Hof 1, 8093 Zurich, Switzerland*
[2]*Université de Neuchâtel, Laboratoire Temps-Frequence, 51 Avenue de Bellevaux, 2000 Neuchâtel, Switzerland*
[3]*These authors contributed equally*
[*]*emaury@phys.ethz.ch*

Abstract: We present a detailed study of the carrier-envelope offset (CEO) frequency dynamics of SESAM modelocked thin disk lasers (TDLs) pumped by kW-class highly transverse multimode pump diodes with a typical M^2 value of 200-300, and give guidelines for future frequency stabilization of multi-100-W oscillators. We demonstrate CEO frequency detection with > 30 dB signal-to-noise ratio with a resolution bandwidth of 100 kHz from a SESAM modelocked Yb:YAG TDL delivering 140 W average output power with 748-fs pulses at 7-MHz pulse repetition rate. We compare with a low-power CEO frequency stabilized Yb:CALGO TDL delivering 2.1 W with 77-fs pulses at 65 MHz. For both lasers, we perform a complete noise characterization, measure the relevant transfer functions (TFs) and compare them to theoretical models. The measured TFs are used to determine the propagation of the pump noise step-by-step through the system components. From the noise propagation analysis, we identify the relative intensity noise (RIN) of the pump diode as the main contribution to the CEO frequency noise. The resulting noise levels are not excessive and do not prevent CEO frequency stabilization. More importantly, the laser cavity dynamics are shown to play an essential role in the CEO frequency dynamics. The cavity TFs of the two lasers are very different which explains why at this point a tight CEO frequency lock can be obtained with the Yb:CALGO TDL but not with the Yb:YAG TDL. For CEO stabilization laser cavities should exhibit high damping of the relaxation oscillations by nonlinear intra-cavity elements, for example by operating a SESAM in the roll-over regime. Therefore the optimum SESAM operation point is a trade-off between enough damping and avoiding multiple pulsing instabilities. Additional cavity components could be considered for supplementary damping independent of the SESAM operation point.

OCIS codes: (320.0320) Ultrafast optics; (140.4050) Mode-locked lasers; (140.3425) Laser stabilization.

References and links

1. H. R. Telle, G. Steinmeyer, A. E. Dunlop, J. Stenger, D. H. Sutter, and U. Keller, "Carrier-envelope offset phase control: A novel concept for absolute optical frequency measurement and ultrashort pulse generation," Appl. Phys. B **69**(4), 327–332 (1999).
2. D. J. Jones, S. A. Diddams, J. K. Ranka, A. Stentz, R. S. Windeler, J. L. Hall, and S. T. Cundiff, "Carrier-envelope phase control of femtosecond mode-locked lasers and direct optical frequency synthesis," Science **288**(5466), 635–639 (2000).
3. A. Apolonski, A. Poppe, G. Tempea, C. Spielmann, T. Udem, R. Holzwarth, T. W. Hänsch, and F. Krausz, "Controlling the phase evolution of few-cycle light pulses," Phys. Rev. Lett. **85**(4), 740–743 (2000).
4. M. Ferray, A. L'Huillier, X. F. Li, L. A. Lompré, G. Mainfray, and C. Manus, "Multiple-harmonic conversion of 1064 nm radiation in rare gases," J. Phys. At. Mol. Opt. Phys. **21**(3), L31–L35 (1988).

5. A. McPherson, G. Gibson, H. Jara, U. Johann, T. S. Luk, I. A. McIntyre, K. Boyer, and C. K. Rhodes, "Studies of multiphoton production of vacuum-ultraviolet radiation in the rare gases," J. Opt. Soc. Am. B **4**(4), 595–601 (1987).
6. A. Cingöz, D. C. Yost, T. K. Allison, A. Ruehl, M. E. Fermann, I. Hartl, and J. Ye, "Direct frequency comb spectroscopy in the extreme ultraviolet," Nature **482**(7383), 68–71 (2012).
7. T. Südmeyer, S. V. Marchese, S. Hashimoto, C. R. E. Baer, G. Gingras, B. Witzel, and U. Keller, "Femtosecond laser oscillators for high-field science," Nat. Photonics **2**(10), 599–604 (2008).
8. T. Eidam, S. Hanf, E. Seise, T. V. Andersen, T. Gabler, C. Wirth, T. Schreiber, J. Limpert, and A. Tünnermann, "Femtosecond fiber CPA system emitting 830 W average output power," Opt. Lett. **35**(2), 94–96 (2010).
9. P. Russbueldt, T. Mans, J. Weitenberg, H. D. Hoffmann, and R. Poprawe, "Compact diode-pumped 1.1 kW Yb:YAG Innoslab femtosecond amplifier," Opt. Lett. **35**(24), 4169–4171 (2010).
10. C. J. Saraceno, F. Emaury, O. H. Heckl, C. R. E. Baer, M. Hoffmann, C. Schriber, M. Golling, T. Südmeyer, and U. Keller, "275 W average output power from a femtosecond thin disk oscillator operated in a vacuum environment," Opt. Express **20**(21), 23535–23541 (2012).
11. U. Keller, K. J. Weingarten, F. X. Kärtner, D. Kopf, B. Braun, I. D. Jung, R. Fluck, C. Hönninger, N. Matuschek, and J. Aus der Au, "Semiconductor saturable absorber mirrors (SESAMs) for femtosecond to nanosecond pulse generation in solid-state lasers," IEEE J. Sel. Top. Quantum Electron. **2**(3), 435–453 (1996).
12. F. X. Kärtner, I. D. Jung, and U. Keller, "Soliton Mode-Locking with Saturable Absorbers," IEEE J. Sel. Top. Quantum Electron. **2**(3), 540–556 (1996).
13. Thales, "Alpha kHz", https://www.thalesgroup.com/en/worldwide/group/lasers.
14. Coherent, "Astrella", https://www.coherent.com.
15. Femtolaser, "RAINBOW", http://www.femtolasers.com.
16. A. Ruehl, A. Marcinkevicius, M. E. Fermann, and I. Hartl, "80 W, 120 fs Yb-fiber frequency comb," Opt. Lett. **35**(18), 3015–3017 (2010).
17. S. Prinz, M. Haefner, C. Y. Teisset, R. Bessing, K. Michel, Y. Lee, X. T. Geng, S. Kim, D. E. Kim, T. Metzger, and M. Schultze, "CEP-stable, sub-6 fs, 300-kHz OPCPA system with more than 15 W of average power," Opt. Express **23**(2), 1388–1394 (2015).
18. J. Rothhardt, S. Demmler, S. Hädrich, J. Limpert, and A. Tünnermann, "Octave-spanning OPCPA system delivering CEP-stable few-cycle pulses and 22 W of average power at 1 MHz repetition rate," Opt. Express **20**(10), 10870–10878 (2012).
19. A. Ozawa, J. Rauschenberger, Ch. Gohle, M. Herrmann, D. R. Walker, V. Pervak, A. Fernandez, R. Graf, A. Apolonski, R. Holzwarth, F. Krausz, T. W. Hänsch, and T. Udem, "High harmonic frequency combs for high resolution spectroscopy," Phys. Rev. Lett. **100**(25), 253901 (2008).
20. A. Diebold, F. Emaury, C. J. Saraceno, C. Schriber, M. Golling, T. Südmeyer, and U. Keller, "62-fs pulses from a SESAM modelocked Yb:CALGO thin disk laser," Opt. Lett. **38**, 3842–3845 (2013).
21. O. Pronin, M. Seidel, J. Brons, F. Lücking, I. B. Angelov, V. L. Kalashnikov, V. Pervak, A. Apolonski, T. Udem, and F. Krausz, "Towards CEP stabilized pulses from a KLM Yb:YAG thin-disk oscillator," in *CLEO/Europe 2013,* (OSA, 2013), pp. CFIE-2.2-Sun.
22. F. Emaury, C. J. Saraceno, B. Debord, D. Ghosh, A. Diebold, F. Gèrôme, T. Südmeyer, F. Benabid, and U. Keller, "Efficient spectral broadening in the 100-W average power regime using gas-filled kagome HC-PCF and pulse compression," Opt. Lett. **39**(24), 6843–6846 (2014).
23. C. J. Saraceno, F. Emaury, C. Schriber, A. Diebold, M. Hoffmann, M. Golling, T. Sudmeyer, and U. Keller, "Toward millijoule-level high-power ultrafast thin-disk oscillators," IEEE J. Sel. Top. Quantum Electron. **21**(1), 106–123 (2015).
24. D. C. Yost, A. Cingöz, T. K. Allison, A. Ruehl, M. E. Fermann, I. Hartl, and J. Ye, "Power optimization of XUV frequency combs for spectroscopy applications [Invited]," Opt. Express **19**(23), 23483–23493 (2011).
25. S. Hädrich, J. Rothhardt, M. Krebs, F. Tavella, A. Willner, J. Limpert, and A. Tünnermann, "High harmonic generation by novel fiber amplifier based sources," Opt. Express **18**(19), 20242–20250 (2010).
26. J. Lee, D. R. Carlson, and R. J. Jones, "Optimizing intracavity high harmonic generation for XUV fs frequency combs," Opt. Express **19**(23), 23315–23326 (2011).
27. J. Aus der Au, G. J. Spühler, T. Südmeyer, R. Paschotta, R. Hövel, M. Moser, S. Erhard, M. Karszewski, A. Giesen, and U. Keller, "16.2-W average power from a diode-pumped femtosecond Yb:YAG thin disk laser," Opt. Lett. **25**(11), 859–861 (2000).
28. C. J. Saraceno, F. Emaury, C. Schriber, M. Hoffmann, M. Golling, T. Südmeyer, and U. Keller, "Ultrafast thin-disk laser with 80 μJ pulse energy and 242 W of average power," Opt. Lett. **39**(1), 9–12 (2014).
29. D. E. Spence, P. N. Kean, and W. Sibbett, "60-fsec pulse generation from a self-mode-locked Ti:sapphire laser," Opt. Lett. **16**(1), 42–44 (1991).
30. J. Brons, V. Pervak, E. Fedulova, D. Bauer, D. Sutter, V. Kalashnikov, A. Apolonskiy, O. Pronin, and F. Krausz, "Energy scaling of Kerr-lens mode-locked thin-disk oscillators," Opt. Lett. **39**(22), 6442–6445 (2014).
31. C. J. Saraceno, S. Pekarek, O. H. Heckl, C. R. E. Baer, C. Schriber, M. Golling, K. Beil, C. Kränkel, G. Huber, U. Keller, and T. Südmeyer, "Self-referenceable frequency comb from an ultrafast thin disk laser," Opt. Express **20**(9), 9650–9656 (2012).
32. A. Klenner, F. Emaury, C. Schriber, A. Diebold, C. J. Saraceno, S. Schilt, U. Keller, and T. Südmeyer, "Phase-stabilization of the carrier-envelope-offset frequency of a SESAM modelocked thin disk laser," Opt. Express **21**(21), 24770–24780 (2013).

33. S. Witte, R. T. Zinkstok, W. Hogervorst, and K. S. E. Eikema, "Control and precise measurement of carrier-envelope phase dynamics," Appl. Phys. B **78**(1), 5 (2004).
34. O. Pronin, M. Seidel, F. Lücking, J. Brons, E. Fedulova, M. Trubetskov, V. Pervak, A. Apolonski, T. Udem, and F. Krausz, "High-power multi-megahertz source of waveform-stabilized few-cycle light," Nat. Commun. **6**, 6988 (2015).
35. L. Matos, O. D. Mücke, J. Chen, and F. X. Kärtner, "Carrier-envelope phase dynamics and noise analysis in octave-spanning Ti:Sapphire lasers," Opt. Express **14**(6), 2497–2511 (2006).
36. A. Schlatter, S. C. Zeller, R. Grange, R. Paschotta, and U. Keller, "Pulse energy dynamics of passively mode-locked solid-state lasers above the Q-switching threshold," J. Opt. Soc. Am. B **21**(8), 1469–1478 (2004).
37. A. Giesen, H. Hügel, A. Voss, K. Wittig, U. Brauch, and H. Opower, "Scalable concept for diode-pumped high-power solid-state lasers," Appl. Phys. B **58**(5), 365–372 (1994).
38. C. J. Saraceno, C. Schriber, M. Mangold, M. Hoffmann, O. H. Heckl, C. R. E. Baer, M. Golling, T. Südmeyer, and U. Keller, "SESAMs for high-power oscillators: design guidelines and damage thresholds," IEEE J. Sel. Top. Quantum Electron. **18**(1), 29–41 (2012).
39. C. Schriber, L. Merceron, A. Diebold, F. Emaury, M. Golling, K. Beil, C. Kränkel, C. J. Saraceno, T. Südmeyer, and U. Keller, "Pushing SESAM modelocked thin-disk lasers to shortest pulse durations," in *Advanced Solid State Lasers*, OSA Technical Digest (online) (OSA, 2014), AF1A.4.
40. M. Haiml, R. Grange, and U. Keller, "Optical characterization of semiconductor saturable absorbers," Appl. Phys. B **79**(3), 331–339 (2004).
41. A. Klenner and U. Keller, "All-optical Q-switching limiter for high-power gigahertz modelocked diode-pumped solid-state lasers," Opt. Express **23**(7), 8532–8544 (2015).
42. R. Grange, M. Haiml, R. Paschotta, G. J. Spuhler, L. Krainer, M. Golling, O. Ostinelli, and U. Keller, "New regime of inverse saturable absorption for self-stabilizing passively mode-locked lasers," Appl. Phys. B **80**, 151–158 (2005).
43. J. M. Dudley, G. Genty, and S. Coen, "Supercontinuum generation in photonic crystal fiber," Rev. Mod. Phys. **78**(4), 1135–1184 (2006).
44. K. W. DeLong, R. Trebino, J. Hunter, and W. E. White, "Frequency-resolved optical gating with the use of second-harmonic generation," J. Opt. Soc. Am. B **11**(11), 2206–2215 (1994).
45. Z. Instruments, "UHFLI", http://www.zhinst.com/products/uhfli.
46. G. Di Domenico, S. Schilt, and P. Thomann, "Simple approach to the relation between laser frequency noise and laser line shape," Appl. Opt. **49**(25), 4801–4807 (2010).
47. R. W. Fox, C. W. Oates, and L. W. Hollberg, "Stabilizing diode lasers to high-finesse cavities," in *Experimental Methods in the Physical Sciences*, D. v. Z. Roger and J. P. Looney, eds. (Academic Press, 2003), pp. 1–46.
48. N. Bucalovic, V. Dolgovskiy, M. C. Stumpf, C. Schori, G. Di Domenico, U. Keller, S. Schilt, and T. Südmeyer, "Effect of the carrier-envelope-offset dynamics on the stabilization of a diode-pumped solid-state frequency comb," Opt. Lett. **37**(21), 4428–4430 (2012).
49. R. P. Scott, T. D. Mulder, K. A. Baker, and B. H. Kolner, "Amplitude and phase noise sensitivity of modelocked Ti:sapphire lasers in terms of a complex noise transfer function," Opt. Express **15**(14), 9090–9095 (2007).
50. C. Hönninger, R. Paschotta, F. Morier-Genoud, M. Moser, and U. Keller, "Q-switching stability limits of continuous-wave passive mode locking," J. Opt. Soc. Am. B **16**(1), 46–56 (1999).
51. S. Schilt, N. Bucalovic, L. Tombez, V. Dolgovskiy, C. Schori, G. Di Domenico, M. Zaffalon, and P. Thomann, "Frequency discriminators for the characterization of narrow-spectrum heterodyne beat signals: application to the measurement of a sub-hertz carrier-envelope-offset beat in an optical frequency comb," Rev. Sci. Instrum. **82**(12), 123116 (2011).
52. T. M. Fortier, J. Ye, S. T. Cundiff, and R. S. Windeler, "Nonlinear phase noise generated in air-silica microstructure fiber and its effect on carrier-envelope phase," Opt. Lett. **27**(6), 445–447 (2002).
53. A. Diebold, T. Zengerle, M. Mangold, C. Schriber, F. Emaury, M. Hoffmann, C. J. Saraceno, M. Golling, D. Follman, G. Cole, M. Aspelmeyer, T. Südmeyer, and U. Keller, "Optimized SESAMs for Kilowatt Ultrafast Lasers," in *CLEO: 2015*, OSA Technical Digest (online) (Optical Society of America, 2015), STu1O.5.
54. M. Hoffmann, S. Schilt, and T. Südmeyer, "CEO stabilization of a femtosecond laser using a SESAM as fast opto-optical modulator," Opt. Express **21**(24), 30054–30064 (2013).
55. C. C. Lee, C. Mohr, J. Bethge, S. Suzuki, M. E. Fermann, I. Hartl, and T. R. Schibli, "Frequency comb stabilization with bandwidth beyond the limit of gain lifetime by an intracavity graphene electro-optic modulator," Opt. Lett. **37**(15), 3084–3086 (2012).

1. Introduction

Optical frequency combs based on modelocked lasers [1–3] have attracted a lot of attention over the last decade due to their broad range of applications. There is a strong interest to extend stabilized frequency combs into the VUV/XUV spectral range via high-harmonic generation (HHG) [4, 5] to enable VUV/XUV spectroscopy [6] and strong field laser physics and attosecond spectroscopy at megahertz pulse repetition rates [7].

Ideal driving sources for HHG with high average photon flux need a challenging combination of short pulse durations (< 100 fs), high pulse repetition rate (> MHz), and high

pulse energy (> 100 µJ), which requires high average power (>> 100 W). These goals can be achieved with the recent progress in ultrafast diode-pumped Yb-doped solid-state laser systems with multi-100-W average output power based on either fiber amplifier systems [8], Innoslab amplifiers [9], or semiconductor saturable absorber mirror (SESAM) modelocked thin disk lasers (TDL) [10]. Here we address another important requirement, which is the carrier envelope offset (CEO) frequency stabilization. The CEO frequency is the modelocked frequency comb offset and determines the offset of the peak of the electric field with regards to the pulse envelope [1]. We believe that passively modelocked diode-pumped Yb-doped TDLs using SESAMs [11] for starting and stabilizing soliton modelocking [12] will ultimately provide the best CEO and timing jitter noise performance.

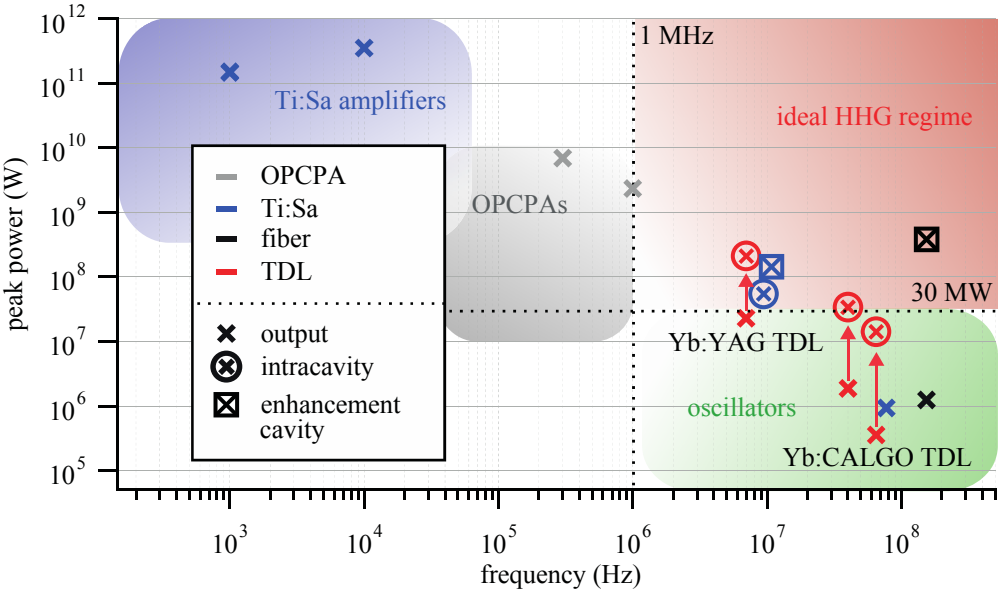

Fig. 1. Overview of peak power and repetition rate of some representative laser systems, including Ti:Sapphire (Ti:Sa) amplifiers [13, 14] and oscillators [15], fiber amplifiers [16], OPCPA systems [17, 18], as well as parameters typically reached inside enhancement cavities [6, 19]. The ideal laser parameters zone for megahertz high-harmonic generation (HHG), e.g. in a gas target, is marked as red-shaded area (f_{rep} > 1 MHz, P_{peak} > 30 MW). In this graph, the trade-off between repetition rate and peak power of currently existing state-of-the-art systems is clearly illustrated. For some current thin disk laser (TDL) results [10, 20, 21], both extra- and intra-cavity parameters are marked in red crosses and crossed circles respectively. Stabilized high-average power frequency combs from TDLs look promising and could also be combined with external pulse compression to further increase the peak power [22].

Although enormous progress has been achieved in the last years in ultrafast sources with high average power from different laser geometries [8, 9, 23], it remains challenging to use them for the direct generation of fully stabilized XUV frequency combs from most standard HHG geometries (i.e. single pass through an external gas target). An alternative approach are stabilized passive enhancement cavities, seeded by high-power amplifier systems [19, 24, 25]. With this approach, the first spectroscopic investigations using a UV frequency comb were recently demonstrated [6], and close to 100 µW per harmonics were achieved in the XUV [26]. An overview of current CEO frequency stabilized high-power sources based on different laser geometries and approaches is presented in Fig. 1. To date, the highest average output power demonstrated from a CEO frequency stabilized laser system is 80 W, obtained from an Yb-doped fiber amplifier with a repetition rate of 154 MHz [16].

SESAM modelocked thin disk lasers (TDLs) [23], are very attractive candidates to reach these and even higher power levels. Since their first demonstration in 2000 [27], TDLs have

achieved higher average powers and pulse energies than any other ultrafast oscillator technology [10, 28]. They reach power levels comparable to amplifier systems [8, 9] from table-top oscillators with reduced complexity. To date, 275 W of average output power in 583-fs pulses [10] and 80-μJ pulse energy in 1.1-ps pulses [28] have been demonstrated with Yb:YAG TDLs. With Kerr lens modelocking (KLM) [29], up to 270 W of average power in 330-fs pulses have been reached [30]. At this point all the multi-100-W average power is achieved with longer pulses in the range of 500 fs to 1 ps. Therefore external pulse compression is required for efficient HHG in an external gas target. High-average-power pulse compression at the hundred watt level to obtain sub-100 fs pulses has recently been demonstrated using Kagome-type hollow-core photonics crystal fibers (PCFs) [22]. In addition, a promising alternative approach is to drive HHG directly inside a TDL resonator generating short pulses [7, 31] similar to the enhancement cavities mentioned above. State-of-the-art TDLs reach sufficient intra-cavity peak powers with sub-100-fs pulse duration [20] (Fig. 1).

One important advantage of TDLs is their intrinsically low noise performance compared to more standard multi-chain amplifier systems. The first demonstration of CEO frequency stabilization of a SESAM modelocked TDL at a moderate output power of 2.1 W was achieved in 2013 [32]. For this result a feedback to the pump laser current was sufficient to phase-lock the CEO beat with a residual phase noise of 120 mrad integrated over a frequency span of [1 Hz; 1 MHz] at a pulse repetition rate of 65 MHz. This proof-of-principle result demonstrated that CEO frequency locking of TDLs is possible despite their highly multimode diode pumping, which was believed to prevent CEO beat locking [33]. Recently, CEO frequency stabilization of a Kerr lens modelocked Yb:YAG TDL was reported at an average power of 17 W [21, 34]. In this case, the 250-fs pulses emitted by the oscillator were externally compressed to < 30 fs and subsequently launched into a photonic crystal fiber and an *f*-to-2*f* interferometer for CEO frequency detection. An intra-cavity acousto-optic modulator was used for CEO beat stabilization, which is a significant challenge for a further increase of the average power and pulse energy. However, despite these promising first proof-of-principle experiments, no thorough investigation of TDL dynamics has been carried out so far. The main challenges to achieve CEO frequency stabilization of systems with hundreds to kilowatts of output power thus remained unclear.

In this paper, we address this question and present a detailed study that provides an in-depth understanding of the trade-offs necessary for CEO frequency stabilization of high-power TDLs pumped by high-power fiber-coupled diodes, using the pump power as an actuator for CEO frequency control and thus keeping the power scalability option. As an important step in this direction, we demonstrate for the first time, to the best of our knowledge, CEO frequency detection of a laser system delivering more than 100 W, based on a SESAM modelocked 140-W Yb:YAG TDL operating at 7 MHz pulse repetition rate. We thoroughly characterize and compare the properties of this 100-W class Yb:YAG TDL to the recently CEO frequency stabilized Yb:CALGO TDL, which operates in a completely different power and pulse duration regime. For both lasers, we perform a complete noise characterization, measure the relevant transfer functions (TF) and compare them to theoretical models [35, 36]. The measured TFs are used to determine the propagation of the pump noise step-by-step through the system components. From the noise propagation analysis, we identify the relative intensity noise (RIN) of the pump diode as the main contribution to the CEO frequency noise power spectral density (PSD) in both TDLs. The resulting noise levels are not excessive and do not prevent CEO stabilization. More importantly, the laser cavity dynamics are shown to play an essential role in the CEO frequency dynamics. Laser cavities exhibiting high damping of the relaxation oscillations by nonlinear intra-cavity elements, for example by operating a SESAM in the roll-over regime, are crucial for a tight CEO beat lock. Our results indicate that fully-stabilized SESAM modelocked TDLs with > 100 W of average

power are in close reach, which would lead to outstanding sources for MHz XUV frequency combs.

The paper is structured as follows. In Section 2, we will present the two laser systems used in this work and describe the CEO beat note detection for each of them. Section 3 will focus on the experimental results. The transfer functions of both laser systems will be discussed in comparison to a theoretical model of cavity dynamics. Furthermore, noise measurements and propagation of the pump noise through the system will be presented, which identifies the pump noise as main contribution to the CEO noise of each laser system. Finally, in Sections 4 and 5, we will present guidelines for the design of high power CEO frequency stabilized TDLs based on our comprehensive study.

2. Experimental set-up

In this study, we compare two laser systems, both SESAM modelocked TDLs. We describe in this section all experimental parameters related to the laser systems and the CEO frequency detection scheme.

2.1 SESAM modelocked thin disk lasers (TDLs)

The TDL concept [37] is based on a thin (typically 50-250 µm) disk-shaped gain material cooled through the backside and used in reflection in the laser cavity. The crystal is optically pumped by a highly multi-mode laser diode, whose output is delivered through a multimode fiber with a typical M^2 value of 200-300. A multi-pass configuration of the pump beam on the disk (see Fig. 2) allows to reach absorption efficiencies > 90% despite a low single-pass pump absorption. Typical pump spot sizes used in this geometry are in the order of a few millimeters radius, resulting in a one-dimensional heat flow. This provides straightforward power scaling capabilities by simply enlarging the pump and laser spot sizes.

We focus here on SESAM modelocked TDLs, which operate in the soliton modelocking regime [12] where the SESAM is starting and stabilizing the modelocking process and the dominant pulse formation is obtained with soliton formation. For this, a high high-damage threshold SESAM [38] is placed as a cavity end mirror.

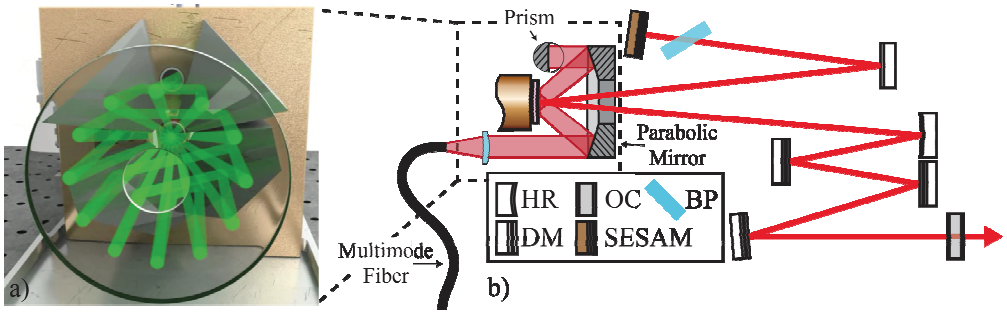

Fig. 2. Schematic of a standard SESAM modelocked TDL. a) Multi-pass thin-disk head, where the pump beam from a multi-mode fiber passes 24 times through the disk [37]. b) Typical TDL cavity with the gain crystal used as folding mirror and the SESAM as an end mirror. HR: high reflectivity mirror, OC: output coupler, BP: Brewster plate, DM: dispersive mirrors, and SESAM: Semiconductor Saturable Absorber Mirror.

2.1.1 Yb:CALGO TDL delivering short pulse duration

The first laser system used in our study is an Yb:CALGO TDL that recently enabled record-short pulses of 62 fs with 5.1 W of average output power [20] and was pushed further to 49 fs and 2.1 W [39]. The first proof-of-principle demonstration of CEO frequency stabilization of a modelocked TDL was achieved using this oscillator [32] in a slightly modified configuration. The details of the oscillator layout can be found in [20]. For the present study, the oscillator delivered 2.1 W of output power at a repetition rate of 64.9 MHz, 77-fs pulse

duration, and an optical spectrum with a full-width at half maximum (FWHM) of 17.1 nm, leading to a time-bandwidth-product (tbp) of 1.14 x sech^2 (Fig. 3). This corresponds to an output pulse energy of 33 nJ and an output peak power of 0.3 MW.

A 223-µm thick Yb:CALGO disk was used as gain medium, which was optically pumped with a commercially available 600-µm fiber-coupled laser diode whose wavelength was stabilized using a volume Bragg grating (VBG). The pump diode (DILAS M1F6L22-979) delivers up to 400 W at a wavelength of 979 nm with an M^2 value of ≈210. The pump diode was driven by a Delta-Elektronika power supply (SM 7.5-80) and was used at a nominal power of 77 W. To achieve stable modelocking, an estimated total dispersion per round-trip of −300 fs^2 was used in combination with a nonlinear phase shift of 240 mrad.

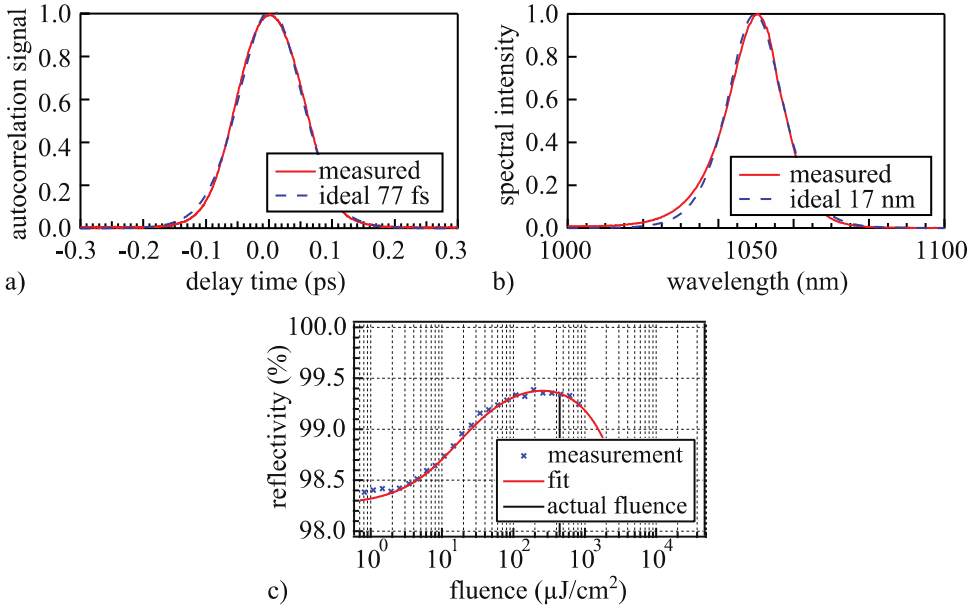

Fig. 3. SESAM modelocked 2.1-W Yb:CALGO laser parameters used in this study. a) Autocorrelation trace (77-fs sech^2-pulses) and b) optical spectrum (17.1 nm FWHM). c) ESAM nonlinear reflectivity curve. A saturation S = 32 was reached on the SESAM at a fluence of 328 µJ/cm^2, when taking into account the Kerr lens in the intra-cavity Brewster plate. At this point of operation, $\partial q / \partial E_s \approx 450\ \mathrm{J}^{-1}$.

The gain and SESAM saturation parameters are very important for the study of the cavity dynamics, which will be presented in Section 3.2. The SESAM parameters were measured at room temperature with 85-fs pulses at a center wavelength of 1050 nm and amounted to F_{sat} = 10 µJ/cm^2 (saturation fluence), ΔR = 1.34% (modulation depth), ΔR_{ns} = 0.50% (non-saturable losses), and F_2 = 275 mJ/cm^2 (induced absorption coefficient). With a spot size diameter of 720 µm on the intra-cavity SESAM and an output coupler of 2.5%, we reached a SESAM saturation parameter $S = F/F_{sat}$ = 32, where F is the intra-cavity fluence. While the saturation parameter S is mostly relevant for the modelocked laser design, the parameter $\partial q / \partial E_S$ is needed to describe the laser dynamics in a model which was first proposed in [35], and which we will use in the following sections for our noise analysis. Here, q is the nonlinear loss of the cavity and E the intra-cavity pulse energy (the subscript S means that the parameter is evaluated in the steady-state condition). We will refer to this parameter $\partial q / \partial E_S$ throughout the rest of the paper. The nonlinear reflectivity of the SESAM represents the main contribution to the nonlinear losses in the cavity [40]. Therefore, it is crucial for our further analysis of the cavity dynamics to properly calculate the exact fluence on the SESAM at the

intracavity operation point used during the experiments. The intra-cavity pulse energy E is related to the SESAM fluence F as $E = F \cdot A_{\mathrm{SESAM}}$, where A_{SESAM} is the laser mode area on the SESAM. A small Kerr lens in the Brewster plate resulted in a reduction of the spot size on the SESAM (≈10%) at the operation point of the laser used for this study. Furthermore, this Kerr lens induces an effective enhanced roll-over of the SESAM as detailed in [41]. Taking into account all these effects at a fixed pulse duration of 77 fs, we calculated $\partial q / \partial E_{\mathrm{S}} \approx 450\ \mathrm{J}^{-1}$ for our Yb:CALGO TDL.

2.1.2 High-power Yb:YAG TDL

The second laser system is a high-power SESAM modelocked TDL based on an Yb:YAG thin disk with a thickness < 100 µm, glued on a water-cooled diamond heat sink. As a pump laser we used a commercially available 1000-µm fiber-coupled laser diode which emits up to 1.2 kW power at a wavelength of 940 nm with an M^2 value of ≈350 (Laserline LDM 1200-60). In our experiment, we operated at a pump power of 566 W. Compared to the pump of the Yb:CALGO laser, the Laserline LDM 1200-60 module combines both the power supply and the diode bars into one box with associated fiber coupling optics.

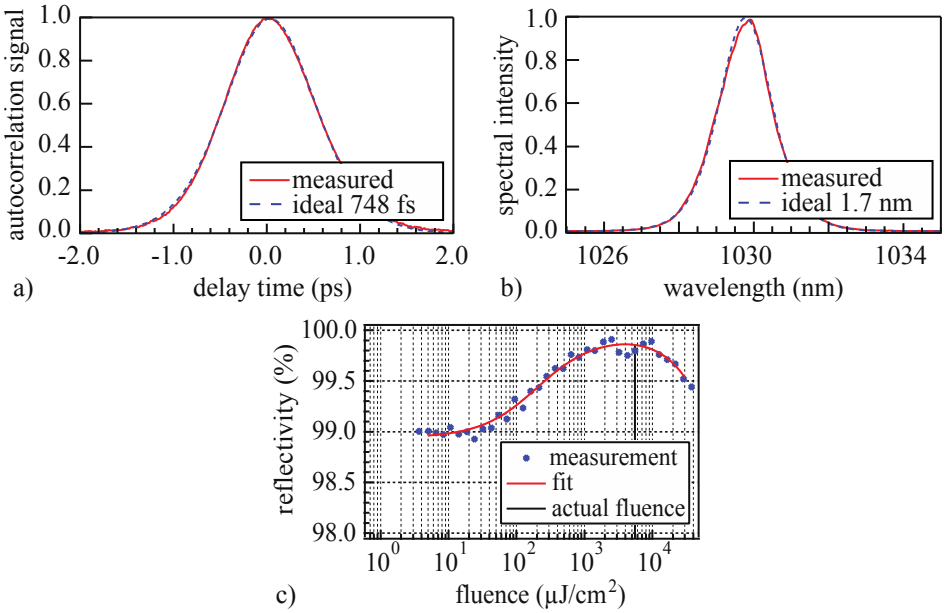

Fig. 4. SESAM modelocked 140-W Yb:YAG laser parameters used in this study. a) Autocorrelation trace of the laser pulse (748-fs sech^2-pulses) b) with its optical spectrum (1.7 nm FWHM). c) A saturation parameter S = 45 was reached on the SESAM at a fluence of ≈5400 µJ/cm^2. At this point of operation, the nonlinear reflectivity curve of the SESAM is nearly flat, corresponding to $\partial q / \partial E_s \approx 2.6\ \mathrm{J}^{-1}$.

The layout of the oscillator is similar to the one that recently showed record-high 275 W average output power [10]. The laser was constructed in a vacuum housing and operated in 150-mbar helium atmosphere at a repetition rate of 7 MHz. The SESAM was designed specifically for high-damage-threshold and high-power operation following the guidelines of [38]. The measured absorber parameters are F_{sat} = 120 µJ/cm^2, ΔR = 1.1%, ΔR_{ns} < 0.1%, and F_2 = 7500 mJ/cm^2, characterized at room temperature with 1-ps pulses at a center wavelength of 1030 nm. For soliton modelocking, we used dispersive mirrors to introduce a total amount of group delay dispersion (GDD) of approximately –11,000 fs^2 per round trip to compensate

for the maximum nonlinear phase of 61.3 mrad. Stable operation over days was achieved with an output power of up to 140 W, at which a pulse duration of 748 fs and a spectrum with a FWHM of 1.5 nm were measured (time-bandwidth products of 1.09 x sech^2) (Fig. 4). This corresponds to an output pulse energy of 20 µJ and an output peak power of 23 MW. With the 11.4% output coupler used in this case, the SESAM is exposed to saturation parameter $S = 45$, which leads to $\partial q / \partial E_S \approx 2.6\ \mathrm{J}^{-1}$, taking into account the increased strength of the rollover parameter F_2 with the slightly shorter pulse duration of our laser [42].

2.2 CEO frequency detection of a TDL

For the CEO frequency detection in a conventional *f*-to-2*f* interferometer [1], we typically need sub-100-fs pulses for the generation of a coherent octave-spanning super-continuum (SC) in a highly nonlinear photonic crystal fiber (PCF) [43]. Depending on the considered laser, a spectral broadening and passive pulse compression stage of a fraction of the output power of the laser is required after the oscillator to reach sufficiently short pulses. These compressed pulses can then be launched into a highly nonlinear PCF to generate an octave-spanning spectrum, followed by CEO beat note detection in a standard *f*-to-2*f* interferometer (Fig. 5, green frame).

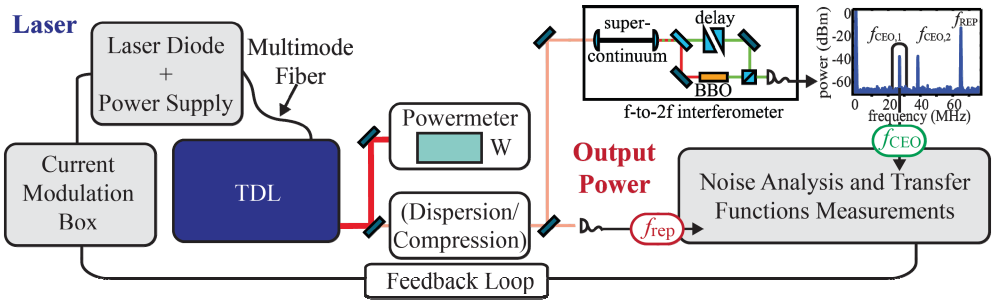

Fig. 5. General experimental setup used in this study. The TDL is pumped by a fiber-coupled diode whose driving current can be modulated via a steering voltage. The output of the laser is split to simultaneously measure its average power, repetition rate f_{rep}, and carrier envelope offset frequency f_{CEO}.

2.2.1 Direct f_{CEO} detection from the Yb:CALGO laser

The Yb:CALGO laser delivers pulses which are sufficiently short for direct coherent SC generation in a highly nonlinear PCF [43]. A small fraction (6%, i.e. 120 mW average power or 2 nJ pulse energy) of the laser output was launched into the *f*-to-2*f*-interferometer, leading to similar performance as previously obtained using a different interferometer [32]. A strong CEO beat note with > 25 dB SNR in a 100 kHz resolution bandwidth (RBW) was reliably detected on a daily basis (Fig. 6). It was usually tuned to 20-30 MHz via the pump power, enabling the use of standard analog band-pass filters and amplifiers to analyze the beat note properties.

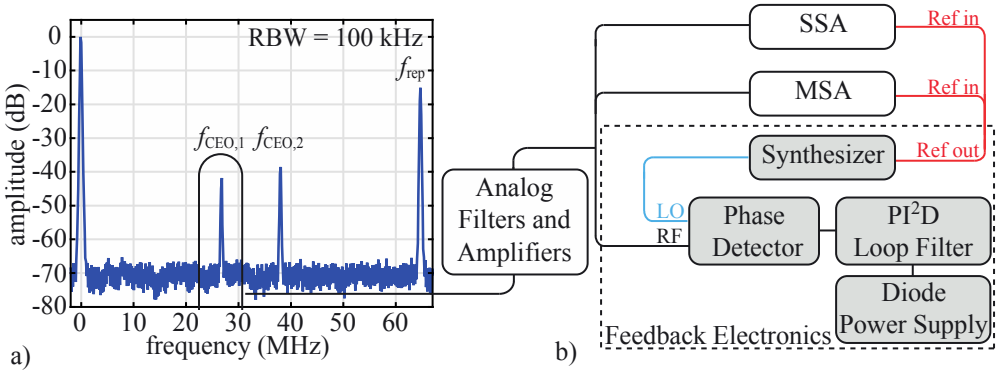

Fig. 6. a) Microwave spectrum of the Yb:CALGO laser output showing $f_{CEO,1}$ and $f_{CEO,2}$ around 27 MHz and 38 MHz for f_{rep} = 64.9 MHz. A resolution bandwidth (RBW) of 100 kHz is used. b) Schematic of the analog electronics setup used for noise analysis and f_{CEO} stabilization of the Yb:CALGO laser (SSA: Signal Source Analyzer, MSA: Microwave Spectrum Analyzer), PI^{2}D: proportional double-integrator derivative servo controller). The feedback signal is sent to the diode power supply to modulate its current.

2.2.2 Pulse compression and f_{CEO} detection from the Yb:YAG TDL

To reach sufficiently short pulses for coherent super-continuum generation, we spectrally broadened a small fraction of the available output power of the oscillator (1%, i.e., 1.5 W, or 200 nJ) using an 8.2-cm long commercially available large mode area PCF (NKT Photonics LMA-PM-10). With a fiber transmission of 60%, the spectrum was broadened to 40 nm FWHM and afterwards recompressed using dispersive mirrors. The optimum compression was achieved at a total dispersion of –11,000 fs^2, introduced via GTI-type dispersive mirrors. The compressed pulses were characterized in a second harmonic generation (SHG) frequency-resolved optical gating (FROG) measurement [44]. The reconstructed *E*-field had a pulse duration of 63 fs FWHM (with a FROG error < 0.005), which was additionally confirmed by a SHG intensity autocorrelation measurement. 70 mW (10 nJ) of the compressed pulses were sent into the PCF of the *f*-to-2*f* interferometer. The high coherence of the generated SC spectrum was experimentally confirmed by the detection of strong CEO beat notes with more than 30 dB SNR in a RBW of 100 kHz (Fig. 7). This is, to our knowledge, the first CEO beat detection of a laser system delivering > 100 W of average output power.

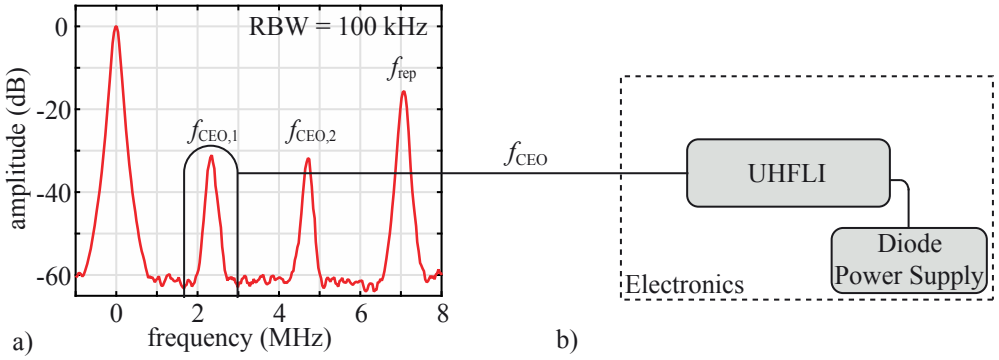

Fig. 7. a) Microwave spectrum of the Yb:YAG laser measured at the output of the *f*-to-2*f* interferometer, showing $f_{CEO,1}$ and $f_{CEO,2}$ around 2.33 MHz and 4.67 MHz, respectively, for f_{rep} = 7 MHz. A resolution bandwidth (RBW) of 100 kHz is used here. b) Schematic of the electronic filtering and demodulation of the CEO beat in the Yb:YAG laser using only the UHFLI in order to perform characterization on the f_{CEO} signal and to apply signal on the pump diode to modulate its current.

In the Yb:YAG TDL, the first CEO beat note $f_{CEO,1}$ lies at a low frequency of around 2.33 MHz. For narrow-band filtering and characterization of this beat signal we used a novel ultra-high frequency digital lock-in amplifier from Zurich Instruments (ZI UHFLI [45]). It encompasses a digital phase lock loop (PLL) that is capable of tracking phase fluctuations of an input signal within a bandwidth of > 500 kHz. Using this digital PLL, the CEO frequency signal was processed to measure its frequency noise PSD. In addition, this device was used to measure transfer functions (Section 3.2) when modulating the pump diode steering voltage.

3. Experimental results

3.1 Bandwidth requirement for CEO stabilization of a TDL

For the design of a feedback loop to achieve a tight CEO frequency lock it is important to estimate the required minimum feedback bandwidth which is independent of the type of feedback loop and actuator used for the stabilization. For this purpose, the frequency noise PSD of the free-running CEO beat note was measured for each laser. For the Yb:CALGO laser we used a frequency discriminator with a fast Fourier transform (FFT) spectrum analyzer in the range from 10 Hz up to 100 kHz. For the Yb:YAG TDL the frequency noise PSD of the CEO beat was measured using the digital PLL of the UHFLI.

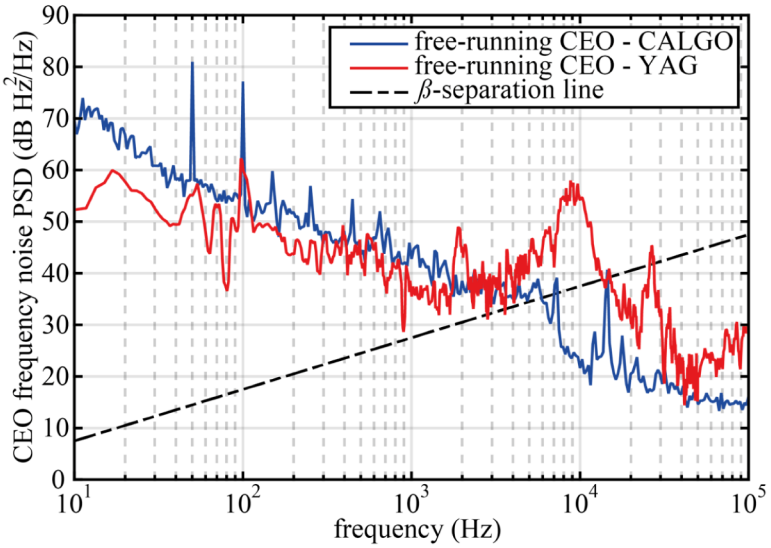

Fig. 8. CEO frequency noise PSD measured for the 2.1-W Yb:CALGO TDL (blue curve) and for the 140-W Yb:YAG TDL (red curve). The β-separation line (black dashed line) was used to estimate the required feedback bandwidth to achieve a tight CEO-lock [46], which is 7 kHz for the Yb:CALGO TDL, and 30 kHz for the Yb:YAG TDL.

Figure 8 shows that the two lasers have a comparable free-running CEO frequency noise PSD even though their laser average output powers differ by nearly two orders of magnitude. A significant difference between the two spectra is the broad resonant noise peak occurring at about 9 kHz in the Yb:YAG laser, whose origin and impact will be discussed in detail later. The similar CEO noise measured for the two lasers are a strong indication that CEO stabilization of a laser with multi-100 W average power is feasible, since CEO stabilization was already demonstrated for the Yb:CALGO system [32]. The minimum feedback bandwidth required to achieve a tight CEO frequency lock was estimated from the crossing point between the CEO frequency noise PSD and the β-separation line, introduced by Di Domenico et al. [46] and displayed in Fig. 8. It corresponds to around 7 kHz for the Yb:CALGO TDL and around 30 kHz for the Yb:YAG TDL. Such a bandwidth can generally be achieved using standard feedback electronics. However, a key aspect is the achievable loop

bandwidth of the actuator used to control f_{CEO}. In particular, the phase response of f_{CEO} is of considerable importance in the ability to phase-lock the CEO beat signal. The overall phase shift induced in the loop must remain far enough below 180° at the unity gain frequency (phase margin) to keep the loop stable [47]. A significant phase shift arising in the response of f_{CEO} to a modulation of the actuator can have a detrimental effect on the possibility to phase-lock f_{CEO} as previously demonstrated in a diode-pumped solid-state laser [48]. Therefore, it is essential to carefully characterize the TFs. Such a characterization performed in our two laser systems is presented in the next Section 3.2.

3.2. Cavity transfer functions (TFs)

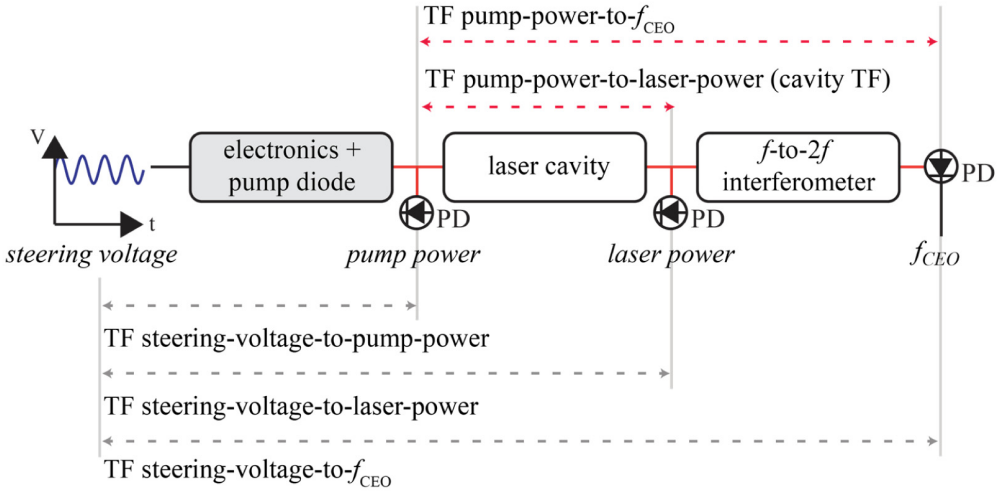

Fig. 9. Measurement principle of the different transfer functions (TFs). PD: photodiode; solid black lines represent electrical connections; solid red lines show optical beams; dashed grey lines represent the electronic input/output signals used for the measured TFs, and dashed red lines represent TFs computed from the measured TFs. The pump-power-to-laser TF (i.e. cavity TF) and pump-power-to-f_{CEO} TF are independent of the pump diode electronics and describe the dynamics of the laser cavity alone.

As shown in Fig. 5, we have for both lasers the possibility to modulate the optical pump power using a steering voltage of the pump power supply. In the case of the Yb:CALGO TDL, a home-made modulation box was used and directly connected to the diode stacks, whereas a commercial solution was used in the case of the Yb:YAG TDL. By modulating the steering voltage, we were able to measure three different TFs (in amplitude and phase), namely of the pump power, the laser output power, and the CEO frequency (Fig. 9).

From these measurements, the TF of the TDL cavity, i.e. the pump-power-to-laser-power TF as well as the pump-power-to-f_{CEO} TF were determined, following and extending the approach previously carried out for a Ti:Sa laser [49] or several Yb:doped lasers [36], where only the pump-power-to-laser-power TF had been determined.

The pump-power-to-laser-power and pump-power-to-f_{CEO} TFs are independent of the pump diode electronics and describe the dynamics of the laser cavities alone. The first one will be subsequently referred to as ‘cavity TF’. The corresponding measurements for the two TDLs are displayed in Fig. 10 and 11. For each laser, these two TFs are very similar, which reveals that the fluctuations of f_{CEO} are linearly coupled to the changes in the laser intra-cavity pulse energy. This outcome is in accordance with general theoretical models applied to Ti:Sa lasers [35]. The minor differences observed in the two TFs of the same oscillator can result from small experimental imprecisions in the measurement of the f_{CEO} TF that was less straightforward to implement than the laser output power.

The cavity TFs of the two lasers are very different. For the Yb:YAG laser (Fig. 11) the cavity behaves like a resonant second-order low-pass filter with a resonance frequency of 7.5 kHz and a quality factor of 4. This resonance appears as a peak in the amplitude accompanied by a 180 degree phase shift occurring in a narrow frequency range. For the Yb:CALGO TDL (Fig. 10), the cavity behaves like a second-order low-pass filter with a pronounced damping (quality factor of 0.15) and a cut-off frequency of around 12 kHz (defined by phase shift –90 deg). In that case, the phase smoothly changes over a broad frequency span of almost three orders of magnitude.

We compared the measured cavity TFs of our lasers to theoretical considerations obtained from intracavity gain and power dynamics that predict a second-order low-pass filter TF from pump power to output power [35, 36]. Following the derivations presented in [35], the following complex cavity transfer function was obtained for modelocked 3- or 4-level laser systems:

$$\frac{\delta P_{\text{out}}}{\delta P_{\text{P}}}(\omega) = \frac{\alpha}{(i\omega)^2 + \left(\beta + \gamma \frac{\partial q}{\partial E_{\text{S}}}\right) i\omega + \epsilon \frac{\partial q}{\partial E_{\text{S}}} + \eta} \qquad (1)$$

Here P_{out} is the laser output power, P_{P} is the pump power, $\alpha, \beta, \gamma, \epsilon,$ and η represent different coefficients depending on basic laser parameters (such as pump power, intra-cavity power, spot size on the laser disk, output coupling rate, total intra-cavity losses, repetition rate, emission and absorption cross sections at the lasing wavelength, and upper state lifetime of the gain medium as detailed in [35]), i is the imaginary number, and ω the angular frequency. Equation (1) represents a second-order low-pass filter with a resonance frequency around the cavity relaxation oscillation frequency. Using the parameters of our two lasers, we adapted the theoretical transfer function with our experimental data with Eq. (1) using the value $\partial q / \partial E_{\text{S}}$ as the only free parameter, as it is the least precisely known quantity. The corresponding theoretical TFs are plotted in Fig. 10 and 11, and show a very good agreement with the measured curves. A low damping factor $\partial q / \partial E_{\text{S}} \approx 3\ \text{J}^{-1}$ was retrieved from the fit for the Yb:YAG TDL, whereas a larger value $\partial q / \partial E_{\text{S}} \approx 4000\ \text{J}^{-1}$ was obtained for the Yb:CALGO TDL, which reflects the strong difference in the damping behavior of the two laser cavities.

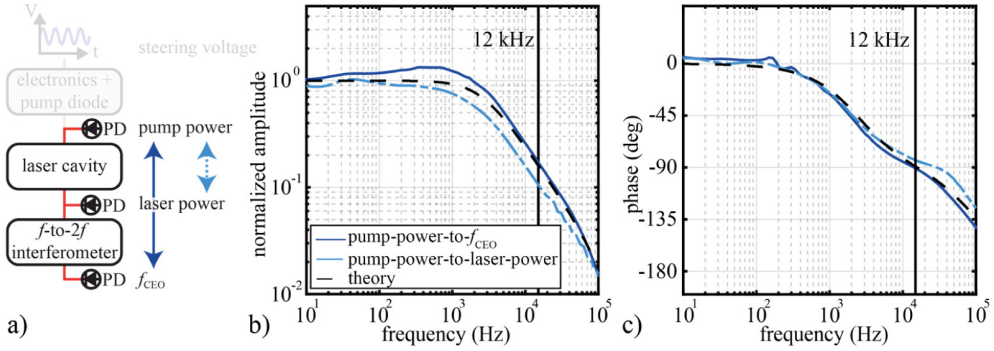

Fig. 10. Transfer functions (TFs) of the Yb:CALGO TDL at its operation point described in Section 2. a) Principle of the TFs measurement. b) Normalized amplitude and c) phase of the TFs. The dashed-dotted blue line represents the measured cavity TF (i.e., pump-power-to-laser-power TF); the solid line displays the measured pump-power-to-f_{CEO} TF; the black dashed line arises from the theoretical model on the cavity dynamic [35] with $\partial q / \partial E_{\text{S}} \approx 4000\,\text{J}^{-1}$. Vertical black lines: resonance frequency of the Yb:CALGO TDL cavity at 12 kHz.

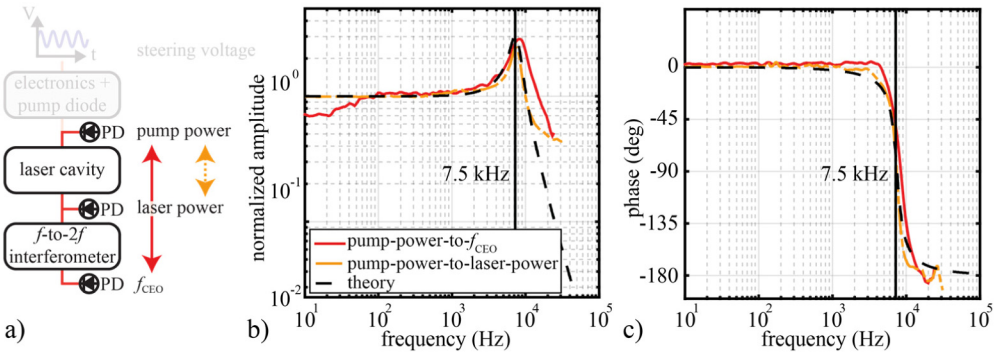

Fig. 11. Transfer functions (TFs) of the Yb:YAG TDL at its operation point described in Section 2. a) Principle of the TFs measurement. b) Normalized amplitude and c) phase of the TFs. The dashed-dotted orange line represents the measured cavity TF (i.e., pump-power-to-laser-power TF); the solid line displays the measured pump-power-to-f_{CEO} TF; the black dashed line arises from the theoretical model on the cavity dynamic [35] with $\partial q / \partial E_S \approx 3\,\mathrm{J}^{-1}$. Vertical black lines: resonance frequency of the Yb:YAG TDL cavity at 7.5 kHz.

The main contribution to the parameter $\partial q / \partial E_S$ in SESAM modelocked TDLs arises from the slope of the nonlinear reflectivity curve of the SESAM at its operation point. Our Yb:YAG laser operates at the maximum of the SESAM nonlinear reflectivity curve, at the beginning of the rollover as observed in Fig. 4, and the parameter $\partial q / \partial E_S$ is consequently estimated to be small ($\approx 2.6\,\mathrm{J}^{-1}$). This value agrees well with the one obtained from the fit of the cavity TF, considering that this factor depends on the SESAM parameters, which can slightly change as a result of the temperature rise induced by the high laser intra-cavity power. The damping term in the cavity TF of our Yb:YAG laser thus results solely from the nonlinear behavior of the SESAM. In the case of the Yb:CALGO TDL, the SESAM operates slightly in the rollover regime (Fig. 3), leading to a value of $\partial q / \partial E_S \approx 450\ \mathrm{J}^{-1}$. The theoretical resonance frequency matches well with the experimental data, but a discrepancy is observed in the value of $\partial q / \partial E_S$ compared to the parameters extracted from the fit of the cavity TF. This discrepancy might arise from a slightly different operation point of the SESAM inside the laser due to temperature induced shifts of the SESAM parameters, or from other nonlinear effects inside the laser cavity. In particular, gain saturation effects due to spectral broadening lead to additional damping terms, which become more dominant the broader the gain spectrum [50]. We estimate this gain-crystal-inherent effect to lead to damping terms smaller or equal to our SESAM damping contribution. Thus, an overall good agreement is observed between the experimentally measured TFs and the fitted curve. In addition, the strong difference observed in the TFs of the two lasers is well explained by the orders-of-magnitude different value of the parameter $\partial q / \partial E_S$.

We therefore assume that our model can be used to predict the behavior of future CEO frequency stabilized kW-class laser oscillators: special attention needs to be taken to optimize the operation point of the SESAM if aiming for CEO beat note stabilization. In particular, it appears that increasing the damping factor by operating the SESAM in the rollover regime is beneficial to smoothen the transfer functions and thus facilitate CEO frequency locking. However, it should be considered that operating the SESAM too deep in the rollover can result in multiple pulsing instabilities and/or damage of the SESAM as shown in [38], so a trade-off set-point needs to be found. SESAM damage should not represent the main limitation, as in [38] it was demonstrated that irreversible damage due to induced absorption occurs only very deep in the rollover regime, where the soliton modelocking stability regime is also not achieved anymore. Additionally, operation slightly above the rollover reduces

long-term SESAM degradation. Therefore, the optimum SESAM operation point is a compromise between enough damping and avoiding multiple pulsing instabilities. Alternatively one may want to consider adding other cavity elements that provide the required damping independently of the operation point of the SESAM.

3.3. Noise origin and propagation

We investigated the origin and propagation of the noise through the two laser systems, starting from pump power fluctuations, and leading to fluctuations of the output power and CEO frequency. This allowed us to understand the origin of the CEO frequency noise, which is important to design a feedback loop to achieve a tight CEO phase lock.

3.3.1 Pump relative intensity noise (RIN)

Out of several potential noise sources in a TDL, we focus here on the optical pump. Environmental influences on laser parameters, such as airflows or vibrations, will not be discussed because they can be reduced by standard engineering. We characterized the relative intensity noise (RIN) of the optical fiber output of the Yb:CALGO TDL pump diode and the Yb:YAG TDL pump diode at the power levels used in our experiments (Fig. 12)

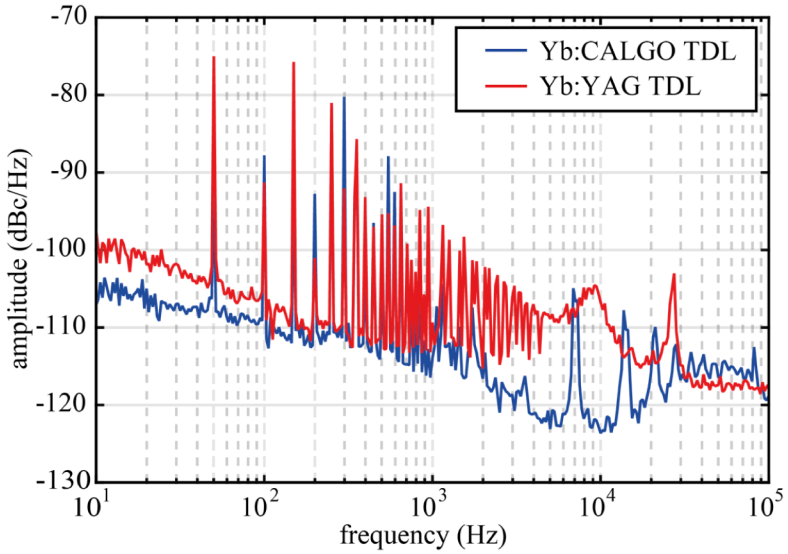

Fig. 12. Relative intensity noises (RIN) of the optical output of the two pump diodes. Integrated root-mean squared (rms) noise is 0.10% [10 Hz; 100 kHz] for the Yb:CALGO TDL pump at 77 W and 0.13% [10 Hz; 100 kHz] for the Yb:YAG TDL at 566 W.

Whereas the 77 W pump beam for the Yb:CALGO laser has an M^2 ≈210 from VBG stabilized diode stacks at 976 nm (FWHM < 0.3 nm), the 566 W pump beam of the Yb:YAG laser has an M^2 ≈350 from non-VBG-stabilized diode stacks at 940 nm (FWHM ≈4-6 nm), making these two pumps very different in terms of their optical properties. However, as shown in Fig. 12, the RIN of these two fiber-coupled diodes is at a very similar level at frequencies below 1 kHz, despite two orders of magnitude difference in their output power. Prominent spikes observed at 50 Hz and harmonics originate from the power supply. At frequencies above 1 kHz, two resonance peaks are clearly visible at 9 kHz and 25 kHz in the RIN of the Yb:YAG TDL pump diode, whereas the RIN of the Yb:CALGO TDL pump diode is reduced at around 10 kHz despite a few high frequency spikes originating from the power supply. It is interesting to note that the pump RINs reveal in this way two main noise components, namely originating from the power supply (spikes) and from multi-mode beating (background). However, a specific study of the different sources of noise in strongly

multimode diodes will not be discussed here, because we want to focus on transfer of these noise properties through our laser systems. The resulting integrated RIN [10 Hz; 100 kHz] is 0.10% for the Yb:CALGO TDL pump at 77 W and 0.13% for the Yb:YAG TDL pump at 566 W, which is remarkably low considering the highly multimode characteristic of these pumps.

3.3.2 Noise propagation through the system

We calculated the propagation of the pump diode RIN through the two laser systems using our measured TFs (Section 3.2). Then, we compared the computed spectra to the measured amplitude noise of the repetition rate carrier and to the frequency noise PSD of the free-running CEO beat for each laser. Figure 13 shows the results for the laser amplitude noise for both laser systems. The computed spectra were simply obtained by multiplying the pump RIN with the respective cavity TF. The measured laser slope efficiencies (5.7% for the Yb:CALGO TDL and 37.5% for the Yb:YAG TDL) were used as a normalization factor. For both Yb:CALGO and Yb:YAG TDLs, the computed curve reproduces all prominent features of the measured spectrum and generally matches it within a reasonable margin, especially for frequencies > 1 kHz and for the integrated noise [10 Hz; 100 kHz], see legend of Fig. 13.

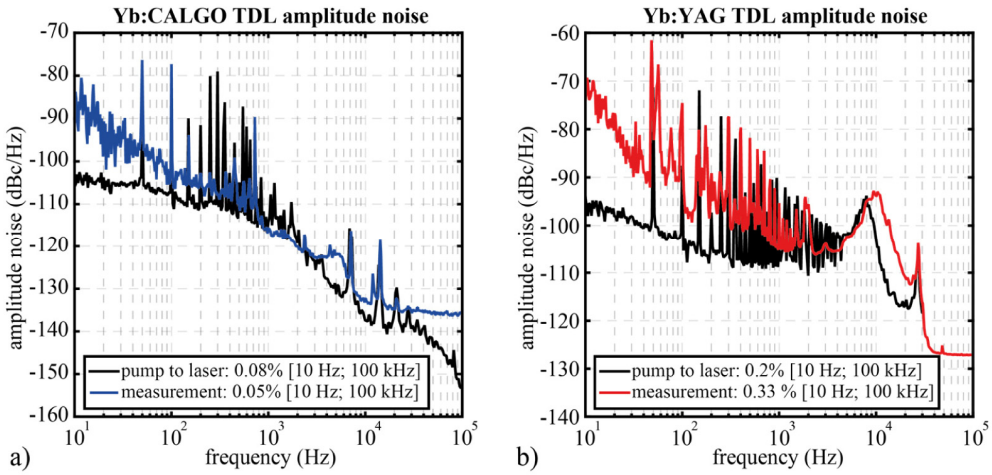

Fig. 13. Measured amplitude noise spectra of the Yb:CALGO TDL (a), blue) and Yb:YAG TDL (b), red) and comparison with the spectra computed from the pump RIN propagation (black curves). Most prominent features of the measured data are reproduced by the computed spectra. The corresponding rms integrated RIN [10 Hz; 100 kHz] is indicated in the legend of each graph.

Additionally, the contribution of the pump RIN to the CEO frequency noise was computed using the pump-power-to-f_{CEO} TF with a normalization factor corresponding to the steady-state frequency shift of the CEO beat measured for a relative change of the pump power (Yb:CALGO TDL: 52.5 MHz/%, Yb:YAG TDL: 26 MHz/%). Figure 14 displays a comparison with the measured CEO frequency PSD, which shows again a good agreement. Both for the laser amplitude noise and CEO frequency noise, discrepancies between the measured and computed noise spectra occur mainly in the low-frequency range (< 100 Hz). These discrepancies originate most likely from environmental influences such as thermal fluctuations or mechanical vibrations, which are more pronounced in the case of the 7-MHz Yb:YAG laser with its 21.4-m long cavity. However, the main features of the measured noise spectra, in particular the peaks at 9.5 kHz and 25 kHz in the Yb:YAG TDL, are well reproduced in the noise computed from the pump RIN propagation. They are particularly interesting because they result from an amplification of the pump noise by the resonant behavior of the Yb:YAG TFs. For the Yb:YAG TDL, the strong noise spikes originating from the power supply, which are clearly observed in the pump RIN (measured with a 1-Hz

resolution), are not visible in the measured CEO frequency noise PSD (Fig. 14(b)) due to the lower spectral resolution of this measurement, performed with the UHFLI instrument (on a linear frequency scale and a 5-Hz resolution). However, these noise spikes are indeed transferred to the CEO noise.

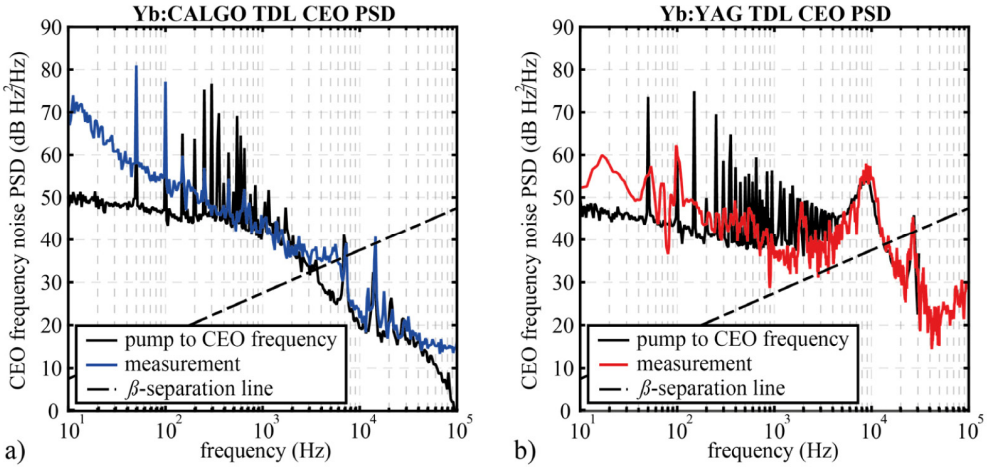

Fig. 14. Measured CEO frequency noise PSD of the Yb:CALGO TDL (a), blue) and Yb:YAG TDL (b), red) and comparison with the spectra computed from the pump RIN propagation (black curves). All prominent features of the measured data are reproduced by the computer spectra. Black-dotted line: β-separation line [46].

The good general agreement obtained between computations and experiments allows us to conclude that the pump RIN constitutes the main contribution to the noise of our laser systems. However, the noise level of these kW-class multimode diodes was revealed in our study to be low, showing comparable integrated values to low power pump diodes. This indicates that although it is the main source of noise, it does not prevent CEO frequency stabilization of TDLs, as demonstrated by our previously achieved stabilization result. In our high-power system, no special attention was paid in the dynamics of the commercially available laser diode.

For future systems, optimized pump diodes with lower noise level operating in the kW-regime will improve residual noise and facilitate CEO beat note locking. For example, optimizing the diode stack bars could be one possible avenue in this direction. A different option would be to attach a notch filter to the pump diode power supply in order to filter its resonance peak, which would subsequently lead to reduced pump RIN, reduced TDL RIN, and reduced CEO frequency noise PSD at resonance. Given, however, that our pump diode is powered by currents > 100 A and voltages of ≈15 V at its point of operation, we believe that designing a stable notch filter for this parameter region would be highly challenging, if not impossible.

Thus, as we pointed out in Section 3.2, the first key milestone will be to achieve appropriate damped cavity TFs in order to reduce the pump-induced CEO frequency noise and especially to create a cavity TF compatible for a feedback loop. We believe this important step alone will allow stabilizing TDLs with current high power diodes available on the market.

4. CEO frequency locking using direct pump modulation and influence of cavity damping

4.1 Successful CEO frequency lock of Yb:CALGO TDL cavity with strong cavity damping

In our previous publication [32] we have demonstrated CEO frequency phase-stabilization of our Yb:CALGO TDL to an external reference. Using direct modulation of the diode current, an in-loop residual integrated phase noise of 118 mrad [10 Hz; 0.1 MHz] and 120 mrad [1 Hz; 1 MHz] was achieved, showing that TDLs can be stabilized despite their highly multimode pumping scheme. We repeated this measurement in the exact laser configuration of the current study, and obtained similar performance with an in-loop integrated phase noise of 163 mrad [10 Hz; 0.1 MHz] (Fig. 15). No out-of-loop measurement of the CEO noise was performed because we had no second similar PCF for SC generation and *f*-to-2*f* interferometer.

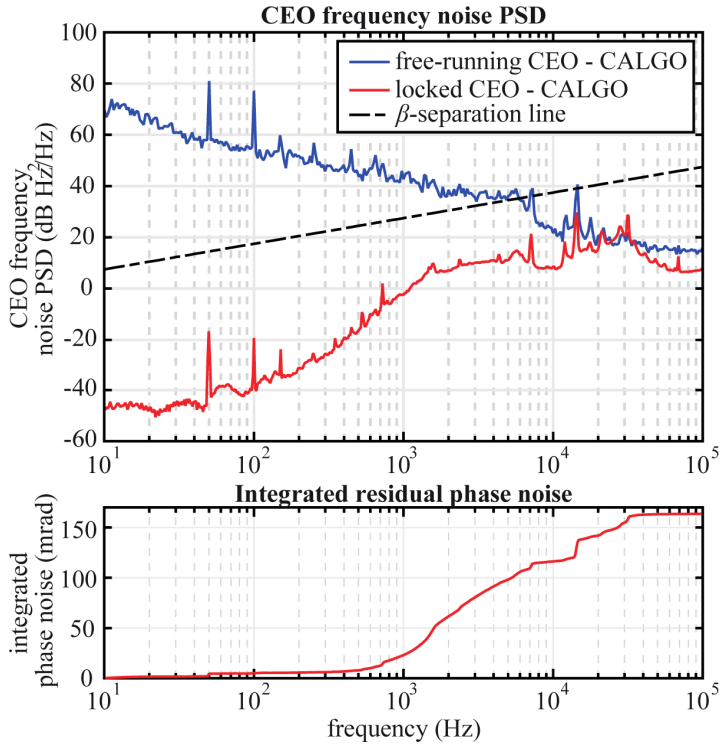

Fig. 15. CEO frequency noise PSD of the Yb:CALGO TDL in free-running (blue curve) and locked (red curve) operation, achieved by direct feedback to the pump diode current. The frequency noise PSD of the locked CEO lies for all frequencies underneath the β-separation line for all frequencies, indicating a tight lock [46].

Recently a 50% difference between the in-loop and out-of-loop integrated phase noise has been reported in a CEO-stabilized Kerr-lens modelocked low-power TDL [34], we are quite confident that an out-of-loop measurement would be less deteriorated in the case of our Yb:CALGO TDL. The difference was partly attributed to amplitude-to-phase (AM-to-PM) noise conversion and partly to the digital phase detector used in the CEO loop. In our case, we carefully checked on one hand the operating point of our digital phase detector according to the observations reported in [51]. On the other hand, we experimentally checked that the amplitude-to-phase noise (AM-to-PM) conversion in the PCF, which is a significant contribution to the extra noise introduced in the generation of the CEO beat [52] had a minor contribution to the integrated phase noise of our stabilized laser with less than 7 mrad [10 Hz;

100 kHz] as obtained as follows. We evaluated the AM-to-PM noise conversion for our Yb:CALGO TDL by applying an amplitude modulation of the light launched into the PCF and measuring the resulting frequency modulation of f_{CEO}. A conversion coefficient of 136 ± 18 mrad/% of the input power variation was obtained. Using the amplitude noise of the Yb:CALGO TDL measured while f_{CEO} was locked, we calculated its contribution to the residual f_{CEO} frequency noise PSD. This induced noise leads to 6.2 mrad [10 Hz; 100 kHz] of integrated phase noise in the in-loop f_{CEO} phase stabilization, which is a minor contribution to the overall integrated phase noise of ≈160 mrad measured for the locked f_{CEO}. This demonstrates that the CEO beat phase stabilization is only marginally affected by the amplitude noise of the laser.

The same stabilization electronics as previously described [32] was used to apply a feedback signal to the diode pump current via the modulation box. As expected from the heavily damped relaxation oscillations TFs measured for this laser (see Section 3.2), a tight CEO frequency lock was straightforward to achieve, owing to the smeared out phase change and damped influence of the pump RIN to the f_{CEO} fluctuations.

This result proves that CEO frequency stabilization is possible for SESAM modelocked TDLs despite their highly multimode pump diodes. Furthermore, the noise propagation analysis presented in this paper shows that f_{CEO} stabilization of this oscillator by direct pump modulation was made possible by the design of a highly damped cavity, combined with appropriate pump diode modulation electronics.

4.2 Challenges for CEO frequency locking of high power TDLs

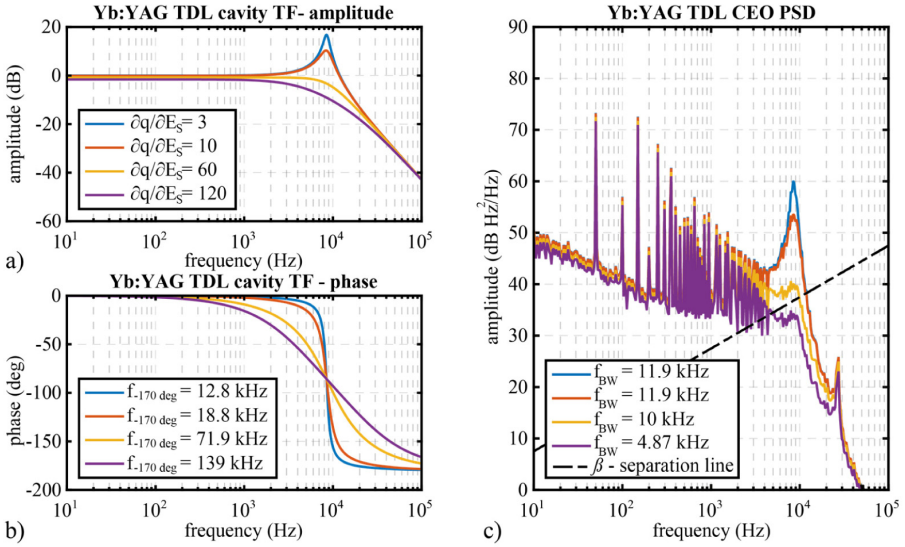

Fig. 16. Cavity dynamics simulations for the Yb:YAG laser at 7 MHz repetition rate and 140 W of output power. While keeping other laser parameters constant, the effect of a higher SESAM damping factor ($\partial q / \partial E_s \approx 3, 10, 60, \text{and} 120\,\text{J}^{-1}$) was simulated to evaluate its influence on the resulting CEO frequency noise. Cavity transfer function (a) in amplitude and (b) in phase for the different damping factors. c) Simulated CEO frequency PSD induced by the measured pump noise. Higher damping factors imply both a reduction of the CEO frequency noise and the simultaneous possibility to further extend the CEO frequency control bandwidth owing to the smaller phase change and damped resonance peak.

CEO stabilization of the Yb:YAG TDL could not be achieved via direct pump modulation. This is a consequence of the abrupt phase change of 180 degrees occurring at 7.5 kHz in the cavity transfer function of this laser (Fig. 11), which typically limits the achievable feedback bandwidth to frequencies lower than this resonance frequency f_{res}. This value is too small

compared to the minimum required feedback bandwidth of at least 30 kHz (as discussed in Section 3.1), needed for tight-locking the CEO beat of the high-power Yb:YAG TDL. Thus, in order to achieve a successful tight lock, the cavity TF needs to be damped to a higher degree in order to reduce the pump RIN resonant contribution to the CEO noise, and to additionally enable the effective feedback bandwidth to be extended beyond the cavity relaxation oscillations frequency.

To illustrate this approach, Fig. 16 shows the impact of the pump RIN onto the CEO frequency noise of the Yb:YAG laser simulated for different SESAM damping factors ($\partial q / \partial E_S \approx 3, 10, 60, \text{and} 120\,\text{J}^{-1}$) while all other laser parameters were kept constant. For this purpose, the measured pump RIN was used as an input signal to compute its contribution to the CEO frequency noise via the cavity TF (see Figs. 16(a) and 16(b)) calculated from Eq. (1) as explained in Section 3.2. By comparing the calculated CEO frequency noise PSD and the achievable CEO frequency control bandwidth assessed from the cavity dynamics, it becomes clear that a higher damping factor is favorable for CEO stabilization by pump power modulation.

5. Guidelines for stabilization of TDLs with > 100 W

Our experimental comparison between two different TDL systems enables us to identify two crucial aspects that need to be tackled towards successful CEO frequency locking of high-power TDLs using pump current modulation as an actuator. The maximum feedback bandwidth achievable with a laser system results from the interplay of pump diode and cavity TF. Pump diodes with flat modulation responses are favorable to increase the CEO frequency control bandwidth as much as possible, but damped cavity designs that enable exceeding the cavity relaxation oscillations are crucial. Thus, two important guidelines were extracted from our analysis:

- Cavity TF: Damped cavities are a prerequisite to achieve the required lock by pump power modulation. Operating the SESAM slightly in the rollover regime is a straightforward way to achieve this. However, operation free of multiple pulsing instabilities needs to be considered: in our most recent energy scaling result [28], we indeed achieved stable modelocked operation with a strongly saturated SESAM (S ≈90). In general, operation at high saturation level can easily be achieved by focusing more tightly on the SESAM. However, operating with extreme intra-cavity powers (>1 kW) and small spot sizes can lead to significant thermally-induced SESAM deformation, which can be detrimental to the modelocked laser resonator in the case of classically-contacted SESAMs (such as the ones we are using for the study presented here). We have recently demonstrated novel SESAM contacting techniques [53], which will allow us to overcome this problem in the near future, therefore facilitating operation at smaller spot sizes without any thermal deformation.
- Influence of pump diode noise: The bandwidth needed for tight f_{CEO} locking is determined by the propagation of the pump RIN via the cavity TF. Therefore, pump diodes with low noise properties are preferable. Our measurements indicate that current kW-class pump diodes achieve sufficiently low noise, comparable to that of standard low-power diodes. Therefore, an appropriate design of the damping of the cavity should provide sufficient improvement to stabilize current multi-100-W TDLs. For future systems, optimization of kW-class pump diodes for low noise operation will also be beneficial to relax cavity design considerations.

6. Conclusion and outlook

The outcome of the reported study allowed us to gain an in-depth understanding of the trade-offs for f_{CEO} stabilization of TDLs pumped by high-power fiber-coupled diodes using

feedback to the pump current. We demonstrated for the first time, to the best of our knowledge, CEO beat note detection of a laser system delivering more than 100 W of average output power. By thoroughly characterizing and comparing the properties of this 140-W Yb:YAG TDL to a recently CEO-stabilized 77-fs Yb:CALGO TDL, first steps towards a full stabilization of a 100-W class TDL via pump diode modulation were presented. For both lasers, we performed a complete noise characterization as well as measurements of all relevant TFs. In particular, we studied the influence of the cavity TF with additional comparison and good agreement to a theoretical model.

The resulting second-order low-pass filter cavity TFs reveal that the two lasers operate in different regimes of relaxation oscillations damping, which is governed by the saturation level on the considered SESAMs. This causes a smooth phase change in the Yb:CALGO TDL and an abrupt 180 degrees phase variation in the high-power Yb:YAG TDL, both centered at the respective relaxation oscillations frequencies. The measured TFs were used to calculate the contribution of the pump RIN to the laser noise in several steps up to the CEO beat note. A good agreement was obtained between the so-calculated noise curves and the experimentally measured spectra, which allowed us to identify the pump diode RIN as the main contribution to the CEO frequency noise in both laser systems.

Our experimental results reveal that f_{CEO} locking in thin disk geometries crucially depends on the damping of the laser cavity. The cavity TF has a direct impact on the magnitude of the noise transferred from the pump RIN to the CEO frequency, thus impacting the feedback bandwidth needed for tight CEO beat note locking. Damped cavities are crucial in this context. As the RIN of the pump diode is the main contribution to the CEO noise in our two systems, the required feedback bandwidth can also be lowered using pump diode lasers with noise levels as low as possible. Additionally, damped cavities are a key point of design because of the increase in the maximum achievable feedback loop bandwidth by a smeared out phase change.

While the influence of pump diode RIN cannot be circumvented, its modulation response could be improved by investigating alternative feedback approaches such as introducing an acousto-optics modulator (AOM) between the pump diode and the gain crystal. This approach, however, introduces a fundamental trade-off between power-handling and modulation bandwidth, which is incompatible with power scaling. Another interesting approach that has recently been demonstrated is the use of the SESAM as an opto-optical modulator [54]. This approach remains to be investigated in the case of TDLs, but is promising as it conserves all power scaling features of TDLs, in contrast to a similar high-speed intracavity actuator using electro-modulated graphene [55], which is more suitable for low power oscillators. Nonetheless, our theoretical understanding of the importance of the cavity TF discussed in Section 3.3 provides us all the necessary tools to design appropriate laser cavities for CEO frequency locking of high-power TDLs.

Given the insights gained by this study, we now can design high-power laser systems which meet all requirements for f_{CEO} stabilization in a wide range of repetition rates. Our precise theoretical knowledge about the cavity TF allows us to adapt our TDLs for improved CEO frequency noise and control bandwidth properties. For the targeted applications, our ultimate goal is to reach CEO beat note stabilization at pulse energies sufficient for HHG at repetition rates in the order of hundreds of MHz and therefore kilowatts of output power.

Acknowledgments

T. Südmeyer acknowledges support by the Swiss National Science Foundation (SNF) (project 146738) and the European Research Council for the project “Efficient megahertz XUV light source” (ERC Starting Grant 2011 #279545). U. Keller would like to acknowledge support by the SNF (project 152967) and the technology and cleanroom facility FIRST of ETH Zurich for advanced micro- and nanotechnology.